Ordering of glass rods in nematic and cholesteric liquid crystals

A. T. Juhl,[1] D.-K. Yang,[2] V. P. Tondiglia,[1,3] L. V. Natarajan,[1,3] T. J. White,[1] and T. J. Bunning[1,*]

[1]*Air Force Research Laboratory, Materials and Manufacturing Directorate, Wright-Patterson Air Force Base, Ohio, 45433, USA*

[2]*Kent State University, Liquid Crystal Institute, Kent, OH 44242, USA*

[3]*Science Applications International Corporation, Dayton, OH 45433, USA*

**Timothy.Bunning@wpafb.af.mil*

Abstract: The orientational assembly of glass rods (3 x ~15 μm) in nematic, twisted nematic, and cholesteric liquid crystal cells was observed and quantified with optical microscopy. At this size, the rods were affected strongly by gravity and sedimented to the bottom of the cells. Temporal visualization of the sedimentation process (induced by flipping the cell over) shed insight into the effect the liquid crystal order had on the glass rod orientation. For nematic and twisted nematic geometries, the glass rods were aligned parallel to the local director orientation. Control experiments indicate that the rod alignment is not due to capillary flow induced artifacts from fabrication of the sample or due to interactions with the buffed substrates. As evidence, the glass rods rotated 90 degrees as they fell from the top to the bottom of a twisted nematic cell. More complex behavior was observed for cholesteric cells depending on the pitch length. A computational model was developed to predict the elastic energy of the system as a function of the angle between the long axis of the glass rod and the cholesteric liquid crystal director. The model predicted that the elastic energy of the system was minimized when the glass rods remained parallel to the cholesteric liquid crystal director when the pitch was sufficiently long, which agrees with experimental results.

©2011 Optical Society of America

OCIS codes: (160.3710) Liquid crystals; (160.1585) Chiral media; (160.2100) Electro-optical materials; (160.0160) Materials.

References and links

1. T. Hegmann, H. Qi, and V. M. Marx, "Nanoparticles in liquid crystals: synthesis, self-assembly, defect formation and potential applications," J. Inorg. Organomet. Polym. Mater. **17**(3), 483–508 (2007).
2. M. D. Lynch and D. L. Patrick, "Controlling the orientation of micron-sized rod-shaped SiC particles with nematic liquid crystal solvents," Chem. Mater. **16**(5), 762–767 (2004).
3. J. D. Mougous, A. J. Brackley, K. Foland, R. T. Baker, and D. L. Patrick, "Formation of uniaxial molecular films by liquid-crystal imprinting in a magnetic field," Phys. Rev. Lett. **84**(12), 2742–2745 (2000).
4. J. B. Pendry, "A chiral route to negative refraction," Science **306**(5700), 1353–1355 (2004).
5. P. R. Evans, G. A. Wurtz, W. R. Hendren, R. Atkinson, W. Dickson, A. V. Zayats, and R. J. Pollard, "Electrically switchable nonreciprocal transmission of plasmonic nanorods with liquid crystal," Appl. Phys. Lett. **91**(4), 043101 (2007).
6. W. Cai, and V. Shalaev, *Optical Metamaterials: Fundamentals and Applications* (Springer Science + Business Media, 2010).
7. L. Cseh and G. H. Mehl, "The design and investigation of room temperature thermotropic nematic gold nanoparticles," J. Am. Chem. Soc. **128**(41), 13376–13377 (2006).
8. L. Li, J. Walda, L. Manna, and P. Alivisatos, "Semiconductor nanorod liquid crystals," Nano Lett. **2**(6), 557–560 (2002).
9. G. N. Karanikolos, N.-L. Law, R. Mallory, A. Petrou, P. Alexandridis, and T. J. Mountziaris, "Water-based synthesis of ZnSe nanostructures using amphiphilic block copolymer stabilized lyotropic liquid crystals as templates," Nanotechnology **17**(13), 3121–3128 (2006).
10. K. Wu, K. Chu, C. Chao, Y. Chen, C. Lai, C. Kang, C. Chen, and P. Chou, "CdS nanorods imbedded in liquid crystal cells for smart optoelectronic devices," Nano Lett. **7**(7), 1908–1913 (2007).

#155093 - $15.00 USD Received 20 Sep 2011; revised 4 Nov 2011; accepted 4 Nov 2011; published 8 Nov 2011

Report Documentation Page

Form Approved
OMB No. 0704-0188

Public reporting burden for the collection of information is estimated to average 1 hour per response, including the time for reviewing instructions, searching existing data sources, gathering and maintaining the data needed, and completing and reviewing the collection of information. Send comments regarding this burden estimate or any other aspect of this collection of information, including suggestions for reducing this burden, to Washington Headquarters Services, Directorate for Information Operations and Reports, 1215 Jefferson Davis Highway, Suite 1204, Arlington VA 22202-4302. Respondents should be aware that notwithstanding any other provision of law, no person shall be subject to a penalty for failing to comply with a collection of information if it does not display a currently valid OMB control number.

1. REPORT DATE	2. REPORT TYPE	3. DATES COVERED
08 NOV 2011		**00-00-2011 to 00-00-2011**

4. TITLE AND SUBTITLE	5a. CONTRACT NUMBER
Ordering of glass rods in nematic and cholesteric liquid crystals	5b. GRANT NUMBER
	5c. PROGRAM ELEMENT NUMBER
6. AUTHOR(S)	5d. PROJECT NUMBER
	5e. TASK NUMBER
	5f. WORK UNIT NUMBER
7. PERFORMING ORGANIZATION NAME(S) AND ADDRESS(ES) **Air Force Research Laboratory,Materials and Manufacturing Directorate,Wright-Patterson AFB,OH,45433**	8. PERFORMING ORGANIZATION REPORT NUMBER
9. SPONSORING/MONITORING AGENCY NAME(S) AND ADDRESS(ES)	10. SPONSOR/MONITOR'S ACRONYM(S)
	11. SPONSOR/MONITOR'S REPORT NUMBER(S)

12. DISTRIBUTION/AVAILABILITY STATEMENT
Approved for public release; distribution unlimited

13. SUPPLEMENTARY NOTES

14. ABSTRACT

The orientational assembly of glass rods (3 x ~15 μm) in nematic, twisted nematic, and cholesteric liquid crystal cells was observed and quantified with optical microscopy. At this size, the rods were affected strongly by gravity and sedimented to the bottom of the cells. Temporal visualization of the sedimentation process (induced by flipping the cell over) shed insight into the effect the liquid crystal order had on the glass rod orientation. For nematic and twisted nematic geometries, the glass rods were aligned parallel to the local director orientation. Control experiments indicate that the rod alignment is not due to capillary flow induced artifacts from fabrication of the sample or due to interactions with the buffed substrates. As evidence, the glass rods rotated 90 degrees as they fell from the top to the bottom of a twisted nematic cell. More complex behavior was observed for cholesteric cells depending on the pitch length. A computational model was developed to predict the elastic energy of the system as a function of the angle between the long axis of the glass rod and the cholesteric liquid crystal director. The model predicted that the elastic energy of the system was minimized when the glass rods remained parallel to the cholesteric liquid crystal director when the pitch was sufficiently long, which agrees with experimental results.

15. SUBJECT TERMS

16. SECURITY CLASSIFICATION OF:			17. LIMITATION OF ABSTRACT	18. NUMBER OF PAGES	19a. NAME OF RESPONSIBLE PERSON
a. REPORT	b. ABSTRACT	c. THIS PAGE			
unclassified	**unclassified**	**unclassified**	**Same as Report (SAR)**	**12**	

11. Q. Liu, Y. Cui, D. Gardner, X. Li, S. He, and I. I. Smalyukh, "Self-alignment of plasmonic gold nanorods in reconfigurable anisotropic fluids for tunable bulk metamaterial applications," Nano Lett. **10**(4), 1347–1353 (2010).
12. H. Chen, C. Chen, C. Wang, F. Chu, C. Chao, C. Kang, P. Chou, and Y. Chen, "Color-tunable light-emitting device based on the mixture of CdSe nanorods and dots embedded in liquid-crystal cells," J. Phys. Chem. C **114**(17), 7995–7998 (2010).
13. T. Lin, C. Chen, W. Lee, S. Cheng, and Y. Chen, "Electrical manipulation of magnetic anisotropy in the composite of liquid crystals and ferromagnetic nanorods," Appl. Phys. Lett. **93**(1), 013108 (2008).
14. C. P. Lapointe, D. H. Reich, and R. L. Leheny, "Manipulation and organization of ferromagnetic nanowires by patterned nematic liquid crystals," Langmuir **24**(19), 11175–11181 (2008).
15. C. Lapointe, N. Cappallo, D. H. Reich, and R. L. Leheny, "Static and dynamic properties of magnetic nanowires in nematic fluids," J. Appl. Phys. **97**(10), 10Q304 (2005).
16. C. Lapointe, A. Hultgren, D. M. Silevitch, E. J. Felton, D. H. Reich, and R. L. Leheny, "Elastic torque and the levitation of metal wires by a nematic liquid crystal," Science **303**(5658), 652–655 (2004).
17. R. Eelkema, M. M. Pollard, J. Vicario, N. Katsonis, B. S. Ramon, C. W. M. Bastiaansen, D. J. Broer, and B. L. Feringa, "Molecular machines: nanomotor rotates microscale objects," Nature **440**(7081), 163 (2006).
18. R. G. Larson, *The Structure and Rheology of Complex Fluids* (Oxford University Press, 1999).
19. R. Barrett, M. Berry, T. F. Chan, J. Demmel, J. Donato, J. Dongarra, V. Eijkhout, R. Pozo, C. Romine, and H. van der Vorst, *Templates for the Solution of Linear Systems: Building Blocks for Iterative Methods*, 2nd ed. (SIAM, 1994).

1. Introduction

Incorporating rod-like particles into liquid crystal (LC) media can lead to self-assembly due to the molecular order of the LC solvent [1]. As rod-like particles are added into the LC, the LC molecules anchor onto the surface of the particle and impose boundary conditions for the LC director. The bulk orientation of the director is distorted to satisfy the surface anchoring conditions which increases the elastic energy of the system. The LC minimizes the elastic energy of the system by imposing a torque on wire, which leads to reorientation. For example, when nanowires were added into a nematic liquid crystal, the wires oriented themselves parallel to the nematic director when the LC had an axial anchoring at the surface of the particle [2]. External forces (i.e. magnetic field) were then used to rotate the LC director orientation and control the orientation of the particles within the system [3].

Particles can be assembled in many LC phases, but the chiral nature of the cholesteric liquid crystal (CLC) is interesting since helical ordering of particles is difficult to achieve by other methods. The ability to helically assemble rods could lead to a system with unique tunable optical properties [4,5]. For instance, helical assembly of nanorods in CLCs could provide a bottom-up approach for fabricating optical metamaterials [6]. As a first step, this paper measures the capability of CLC phases to orientationally order micron-sized glass rods, and a theoretical model is provided to explain the results. Gravitational forces cause sedimentation of the glass rods, and the orientation of the rod as it falls through the thickness of the helical CLC is measured.

As discussed by Hegmann *et. al* [1], there are at least four distinct methods of assembling nano- or micro- sized particles within LC media: LC mesogens can be functionalized onto the surface of the particle [7], anisotropic nanoparticles can be used as the mesogenic units that make up the LC [8], particles can be fabricated within an oriented template of a lyotropic LC [9], or particles can be added into a LC 'solvent' and the elastic forces within the LC can orient the particles [2]. The effort described here focuses on the final method, specifically with rod-shaped particles. There are numerous papers which discuss the assembly of anisotropic particles in nematic liquid crystals [2,3,5,10–14], a few of which have studied the orientation of rod-like particles within twisted-nematic cells [15,16]. To our knowledge, there is no prior analysis on the intricacies of the orientation of rod-like particles incorporated into CLC solvents. However, there is a report of adding glass rods onto photoresponsive CLC films with a fingerprint texture that shows novel results [16]. The pitch of the CLC helix was deformed through UV light exposure, causing the glass rod on the surface of the film to rotate as a molecular motor [17].

In the work presented here, glass rods with 3 μm diameter and an average 15 μm length (actual varied from 10 to 30 μm) were added into nematic, twisted nematic, and CLC cells of differing thickness, and in all cases, the cells were aligned with polyimide buffing layers. The

#155093 - $15.00 USD Received 20 Sep 2011; revised 4 Nov 2011; accepted 4 Nov 2011; published 8 Nov 2011
(C) 2011 OSA

initial orientation of the rods in each sample was quantified with optical microscopy. Since the cell thickness was larger than the thickness of the glass rod spacers, the rods were found to be subject to gravitational forces and accordingly rested on the bottom of the cells. Excluding elastic forces from the LC, gravitational forces on the glass rods will overcome Brownian forces when

$$a^4 \Delta\rho g > k_B T$$

where a is the radius of the particle, $\Delta\rho$ is the density difference of the particle and the solvent, g is 980 cm/sec^2, k_B is Boltzmann's constant and T is temperature [18]. With a 2.57 g/cm^3 rod density and a LC density of approximately 1.03 g/cm^3, the gravitational force on the rods is much larger than the Brownian force, so the glass rods sediment. After settling for 1.5 hours, the LC cells were turned over (the bottom of the cell became the top) and the rod orientation was captured as a function of time as the rods fell through the thickness of the sample. The long axis of the glass rod was always parallel to the director orientation in nematic and twisted nematic cells. To always remain parallel to the director orientation at a specific z-plane in the twisted nematic cell, the rod rotated as it sedimented, feeling the local LC orientation. For CLC samples, the degree of reorientation depended on the pitch of the mixture. A computational model was developed to determine the CLC elastic forces on the glass rod, and results were compared to experimental data. The model correctly predicted that the elastic energy of CLC systems (CLC pitch from 3 to 30 μm) was minimized when the long-axis of the glass rod was parallel to the LC director, and it predicted that there is a larger driving force for rod reorientation as the CLC pitch is increased.

2. Experimental procedure

The nematic liquid crystal mixtures examined here employed commercially available host material, E7. The chiral dopant, CB15 was added to E7 to form CLC mixtures with pitches ranging from 331 nm, 2 μm, 10 μm, 16.6 μm, and 30.7 μm at 41.4, 6.8, 1.36, 0.87 and 0.45 w% (CB15 in E7) respectively. Glass rods with 3, 33, and 50 μm diameter were purchased from Nippon Electric Glass Co. Ltd. (Japan) and were used without modification. LC alignment cells were self-prepared by coating two glass slides with polyimide (HD Microsystems PI2555) followed by rubbing. In the case of the nematic and CLC mixtures examined here, the orientation of the rubbing direction of the two slides was antiparallel. However, to form the twisted nematic orientation, the rubbing direction of the slides was orthogonal. The cell thickness was controlled by mixing 0.01 g of glass rod spacers (either 33 or 50 μm diameter glass rods, as specified) into Norland Optical Adhesive 68 (NOA68). The prepared glass slides were then sealed by spreading this mixture onto two opposite edges of a single slide followed by UV-light exposure to polymerize the NOA68 thereby setting the thickness of the cell to the glass spacer diameter. The cell was then filled with the nematic or CLC mixtures containing the 3 μm glass rods by capillary filling.

Polarizing optical micrographs were taken on a Nikon optical microscope between crossed polarizers. The number of rods in each micrograph and the orientation of the rods were determined using ImageJ software. Laser scanning confocal microscopy was used to measure the rod location within the z-axis of the CLC cells. Data was taken with the BioRad Radiance 2000MP confocal system using a continuous wave 457 nm laser. An image was taken every 0.5 μm in thickness and over an entire thickness of 50 μm.

#155093 - $15.00 USD Received 20 Sep 2011; revised 4 Nov 2011; accepted 4 Nov 2011; published 8 Nov 2011
(C) 2011 OSA

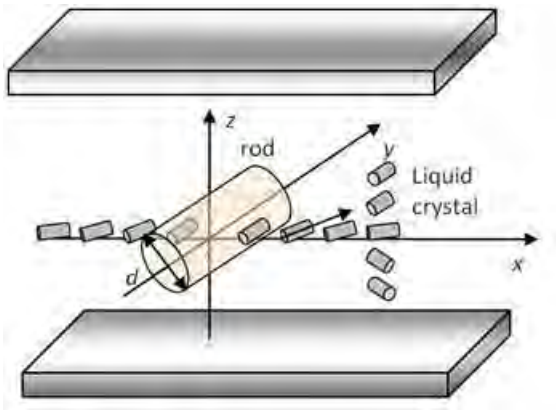

Fig. 1. Schematic of a glass rod in a CLC cell.

A Fortran-based code was used to model the elastic energy of the CLC per unit length of the glass rod. The Frank elastic energy was used to determine the elastic energy of the glass rod in the CLC:

$$f = \frac{1}{2}K_{11}(\nabla \cdot \vec{n})^2 + \frac{1}{2}K_{22}(\vec{n} \cdot \nabla \times \vec{n} + 2\pi / P)^2 + \frac{1}{2}K_{33}(\vec{n} \times \nabla \times \vec{n})^2$$

where f is the elastic energy density, $\vec{n}$ is a vector describing the bulk LC orientation, P is the helical pitch and K_{11}, K_{22}, and K_{33} are the splay twist, and bend elastic constants. The coordinate system was chosen in such a way that the z-axis was along the cell normal direction, the x-axis was perpendicular to the glass rod and the y-axis was parallel to the rod. (Fig. 1) The rod was assumed to be located in the middle of the two substrates. The boundary conditions were defined by the orientation of the LC on the surface of the substrate and on the surface of the rod. On the surface of the glass rod, the LC was aligned parallel to the long axis of the rod. On the inner-surface of the substrates of the cell, the LC was aligned in the planar state by the alignment layer. In the calculation, an infinitely strong anchoring condition was used. In the x-direction, 10 μm away from the glass rod, the LC was assumed to be in the perfect cholesteric planar state. The rod was assumed to be infinitely long so the end effects of the glass rod were neglected. The total elastic energy per unit length (per micron) along the rod was:

$$F = \int_{-h/2}^{h/2} \int_{-L/2}^{L/2} f(x,z)dxdz$$

where the glass substrates are $z = -h/2$ and $z = -h/2$, and the horizontal boundaries are $x = -L/2$ and $x = -L/2$ $(L = h)$. Because the LC director rotates more than 180° in the bulk, it is better to use the tensor representation of the LC director in order to prevent the problem of anti-parallel orientation of the LC director at two neighboring lattice sites in the simulation. In the calculation of the elastic energy we use the $\vec{\vec{Q}}$ tensor defined by

$$\vec{\vec{Q}}(x,y,z) = \vec{n}\vec{n} - \frac{1}{3}\vec{\vec{I}}$$

where $\vec{\vec{I}}$ is the 3x3 identity tensor. Under the tensor representation, the elastic energy is given by

#155093 - $15.00 USD Received 20 Sep 2011; revised 4 Nov 2011; accepted 4 Nov 2011; published 8 Nov 2011
(C) 2011 OSA

$$f = \frac{1}{12}(-K_{11} + 3K_{22} + K_{33})G_1 + \frac{1}{2}(K_{11} - K_{22})G_2 + \frac{1}{4}(-K_{11} + K_{33})G_6 - (2\pi / P)K_{22}G_4$$
$$+ \frac{1}{12}(-K_{11} + 3K_{22} + K_{33})\nabla \cdot (\vec{n}\nabla \cdot \vec{n} + \vec{n} \times \nabla \times \vec{n})]$$

The G_i $(i = 1, 2, 4, 6)$ are defined by $G_1 = \frac{\partial Q_{jk}}{\partial x_l}\frac{\partial Q_{jk}}{\partial x_l}$, $G_2 = \frac{\partial Q_{jk}}{\partial x_k}\frac{\partial Q_{jl}}{\partial x_l}$, $G_4 = e_{jkl}Q_{jm}\frac{\partial Q_{km}}{\partial x_l}$, $G_6 = Q_{jk}\frac{\partial Q_{lm}}{\partial x_j}\frac{\partial Q_{lm}}{\partial x_k}$. In the simulation, a 200×200 mesh is imposed on the area of $20 \times 20\ \mu m^2$ around the rod. The LC director configuration in the equilibrium state is calculated using the over-relaxation method [19].

3. Results and discussion

3.1 Polarization optical microscopy

A nematic liquid crystal containing 3 μm thick glass rod spacers was drawn into a 33 μm thick alignment cell and observed between cross polarizers. Spatial variations in the LC director orientation are displayed as color changes in the polarizing optical microscope. Figure 2(a) is an optical micrograph of a glass rod with the long axis parallel to the rubbing direction of the sample cell. The LC around the rod was black which suggests the LC on the surface of the rod took on an orientation parallel to the long axis of the glass rod. Figure 2(b) is an optical micrograph of a glass rod whose long axis was approximately 34 degrees off the rubbing direction of the sample cell. The LC around the rod is white while the background remains black suggesting that the orientation on the surface of the rod remains parallel to the long axis of the rod while the bulk of the LC remains oriented in the rubbing direction. This disruption of the LC director field imparts forces onto the glass rod that will subsequently be examined in the following experiments.

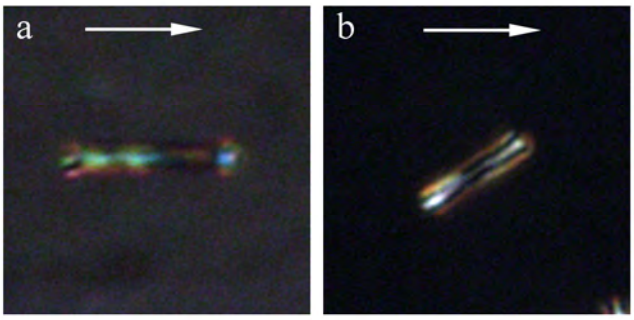

Fig. 2. Polarizing optical micrograph of a (a) glass rod with long axis parallel to the rubbing direction of the sample cell (b) glass rod with long axis 34 degrees from the rubbing direction of the sample cell. In each micrograph the polarizer was parallel to the rubbing direction while the analyzer was perpendicular to it. Note: the exposure time for photograph (a) is longer than that of (b).

3.2 Rods in the nematic phase

Previous studies indicate that the glass rods will take on an orientation parallel to the bulk LC director orientation in nematic liquid crystal [2]. Figure 3(a) confirms that in our model system, the glass rods do indeed take on an orientation parallel to the rubbing direction of the sample cell. The glass rods in the micrograph were resting on the rubbing layer of the bottom substrate. Figure 3(b) quantifies the angular orientation of each rod in the optical micrograph using the program ImageJ. –90 and + 90 degrees are degenerate cases for rods aligning

#155093 - $15.00 USD Received 20 Sep 2011; revised 4 Nov 2011; accepted 4 Nov 2011; published 8 Nov 2011
(C) 2011 OSA

perpendicular to the rubbing direction, while 0 degrees corresponds to a rod that was oriented parallel to the rubbing direction of the cell. Over 80% of the rods were aligned within ± 20° of the buffing direction. It is important to note that glass rods in isotropic medium (water) drawn into a LC cell did not align along the rubbing direction, confirming that elastic forces within the LC were responsible for the ordering of the rods, not the grooves in the buffing layer (Fig. 4).

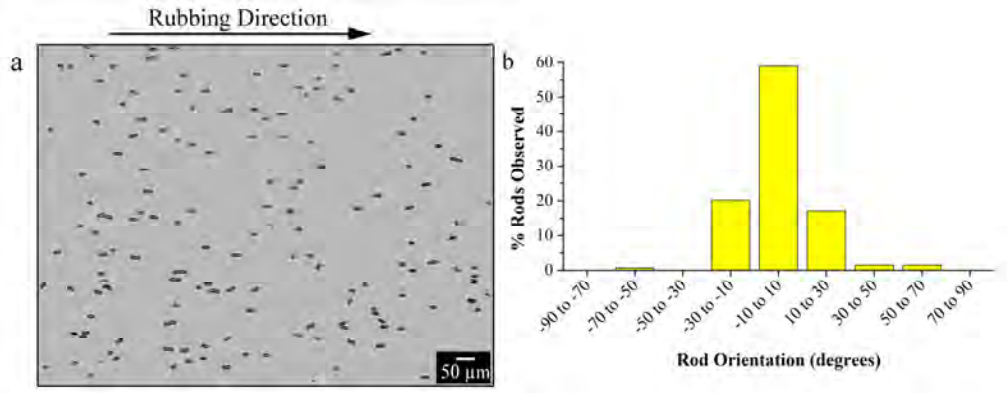

Fig. 3. (a) Optical micrograph of glass rods in nematic liquid crystal E7. Arrow denotes rubbing direction. (b) Histogram quantifying the angular orientations of the glass rods in (a) using ImageJ.

The driving force for the angular rod orientation is described in many references [15]. The bulk LC orientation within the cell was set by the rubbing layers, but another boundary condition was imposed by the parallel anchoring of the LC on the surface of the rod. As the LC anchors parallel to the long axis of the rod, LC molecules that are not on the surface of the rod must distort from their bulk positions to incorporate the new boundary. This distortion puts a torque on the rod that rotates it parallel to the rubbing direction, and minimizes the elastic energy of the system. Rods can also be engineered to align perpendicular to the rubbing direction by altering the anchoring orientation of the LC on the rod [2].

Fig. 4. Optical micrograph of glass rods dispersed in water in an anti-parallel rubbed cell.

To determine that the driving force for glass rod assembly was truly from the elastic forces within the LC, and not just from capillary flow when filling the cell, the same experiment was performed in a circularly rubbed cell. The polyimide layer on each side of the cell was rubbed using a spin coater, so that the director orientation was not in the same direction as the LC capillary flow into the cell. (Fig. 5(a)) There were two defect lines present in the center of the cell due to the circular rubbing, but outside of those lines, the rods had the same circular orientation as the E7. The rods were resting on the buffed bottom substrate. Figure 5(b) presents a histogram quantifying the angular orientation of the rods in the circularly rubbed

#155093 - $15.00 USD Received 20 Sep 2011; revised 4 Nov 2011; accepted 4 Nov 2011; published 8 Nov 2011
(C) 2011 OSA

cell. The rods were aligned almost equivalently in all orientations as would be expected for circular rubbing. The alignment of the rods was due to the elastic forces within the cell and not due to alignment by flow from capillary filling.

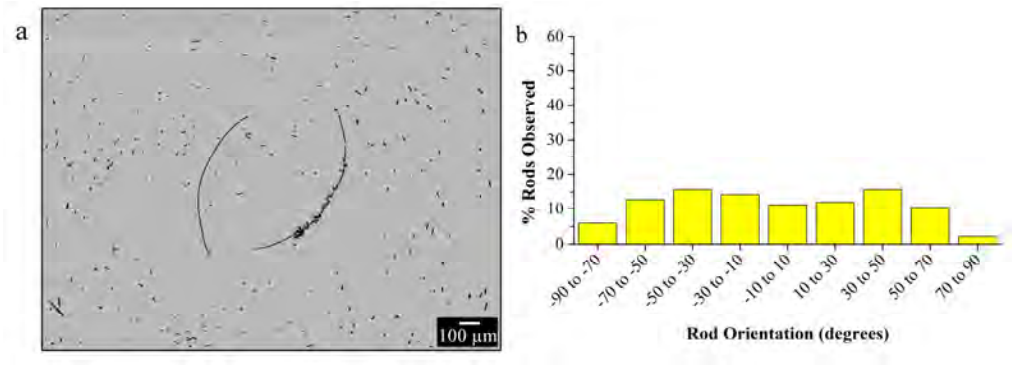

Fig. 5. (a) Optical micrograph of glass rods in a circularly rubbed nematic liquid crystal E7. (b) Histogram quantifying the angular orientations of the glass rods in (a) using ImageJ.

The nematic glass rod mixture was subsequently drawn into a twisted nematic cell to examine the influence of twist in the nematic director on the orientation of the glass rods. Due to gravity, the glass rods resided on the bottom of the cell. When the cell was flipped over (the bottom substrate became the top substrate), gravity acts on the rods, forcing them to the bottom substrate, and allowing the alignment of the glass rods to be monitored as a function of director orientation throughout the cell thickness. Figure 6 is a time sequence of optical micrographs showing the orientations of the rods after the cell has been flipped over. The rods remain aligned parallel to the local in-plane director orientation as they fell through the thickness of the cell.

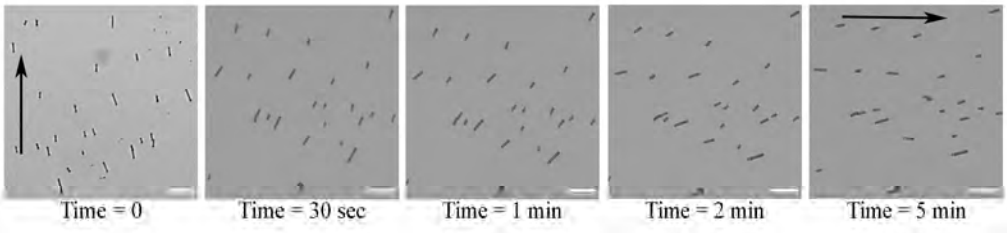

Fig. 6. A series of optical micrographs depicting the orientation of glass rods in a twisted nematic cell as a function of time after it has been flipped over. The scale bar is 50 microns. Arrows denote the rubbing direction of the bottom substrate. Each rod reorients a total of 90 degrees.

3.3 Rods in the cholesteric phase

Cholesteric liquid crystals (CLCs) have a helicoidal orientation of the liquid crystalline director. The distance over which the director of the CLC rotates a full 360° is referred to as the pitch of the CLC. Figure 7(a) presents optical micrographs of 3 µm glass rods in CLCs with a pitch equal to 30.7, 16.6, 10, and 2 µm respectively. Figure 7(b) quantifies the angular orientations of the glass rods in the CLC cells. Each CLC cell was filled and left undisturbed for 1.5 hours before capturing an optical micrograph. Interestingly, the glass rods in CLCs with pitches greater than 30.7 µm (approximately one 360° rotation of the director throughout the cell) tend to take on a specific angular orientation that is not the orientation of the rubbing direction. As the pitch was decreased the rods lost their orientational order.

#155093 - $15.00 USD Received 20 Sep 2011; revised 4 Nov 2011; accepted 4 Nov 2011; published 8 Nov 2011
(C) 2011 OSA

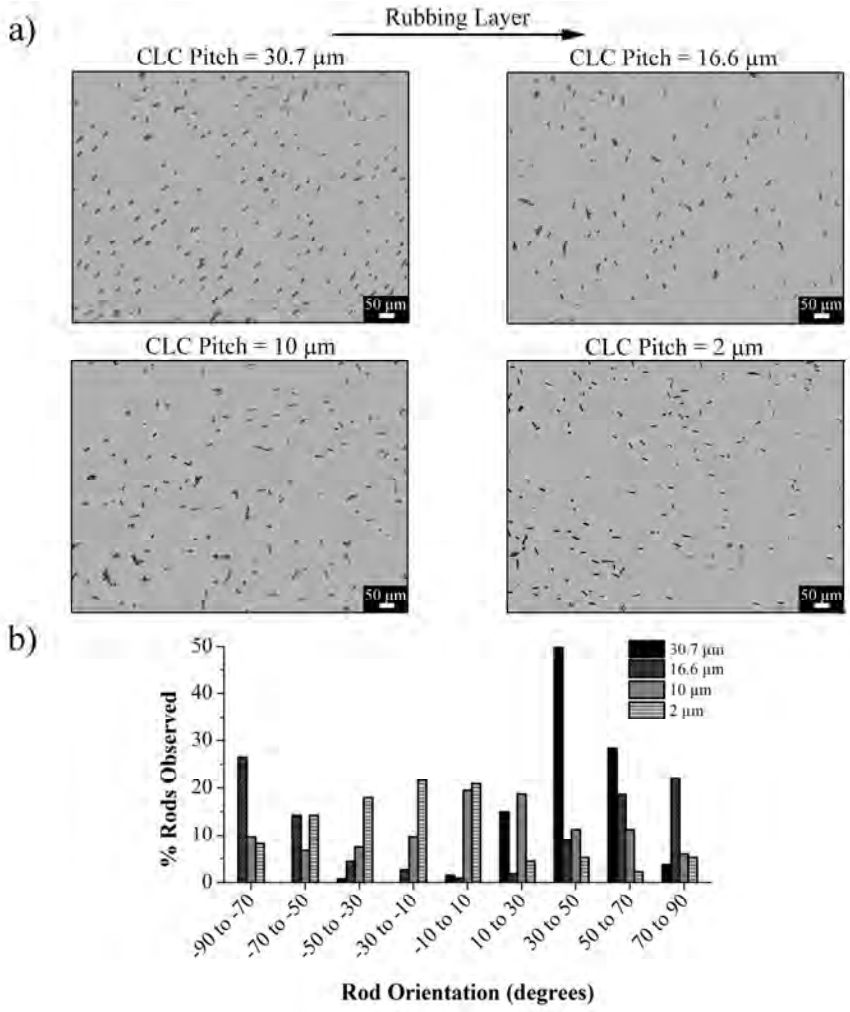

Fig. 7. (a) Optical micrographs of static 3 µm diameter glass rods in 30.7, 16.6, 10, 2 µm pitch cholesteric liquid crystals (CB15/E7). The black arrow denotes the rubbing direction. The scale bars are 50 microns. (b) Histogram quantifying the angular orientations of the glass rods in (a).

The fact that the glass rods were oriented in pitches larger than 30.7 µm can be explained with the same mechanism as for the nematic liquid crystal: the elastic energy of the system was minimized by removing distortions in the LC through rotation of the rod. However, the rods were not oriented in the rubbing direction as they were in the twisted nematic experiment. In the twisted nematic cell, there was a 90° rotation in the LC director through a 50 µm thickness. The CLC with 30.7 µm pitch rotated 360° over the thickness. The 3 µm diameter of the glass rod cannot be neglected in the 30.7 µm pitch CLC samples, because the director orientation rotated by 35 degrees over the radius of the particle, and the lowest energy state of the rods may not be along the rubbing direction.

CLC pitches smaller than 30.7 µm did not show orientational alignment of the rods in a static optical micrograph. As the CLC pitch approached the diameter of the glass rod, the director widely varied its orientation over the thickness of the rod, and the torsional force was averaged out. Each cell was flipped over so that the bottom substrate became the top substrate, and the orientation of the rods was monitored as a function of time as the glass rods migrated through the thickness of the cell (Fig. 8). If the glass rods follow the helical pitch of the LC, rotation of the rods can be expected as they fall along the z-axis of the cell. Figure 8 shows

#155093 - $15.00 USD Received 20 Sep 2011; revised 4 Nov 2011; accepted 4 Nov 2011; published 8 Nov 2011
(C) 2011 OSA

that in the case of the 30.7, 16.6, 10, and 2 µm pitches, the rods rotated as they fell through CLC, indicating that they followed the LC director orientation even though they appear disordered in the static optical micrographs (Fig. 7(a)). Figure 9 contains a series of optical micrographs showing the orientation of a 3 x 22 µm glass rod in a 10 µm pitch CLC cell as a function of time after the cell has been flipped over.

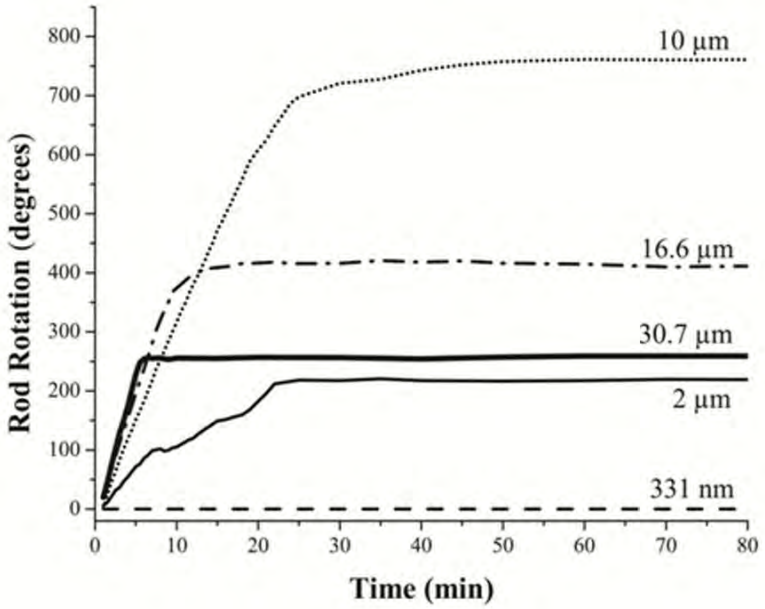

Fig. 8. The number of degrees a 3 µm x 22 µm glass rod rotates in a 30.7, 16.6, 10, 2, and 0.331 µm pitch CLC (CB15/E7) versus time after the cell has been turned over (bottom of the cell becomes the top and the rods are subject to gravity).

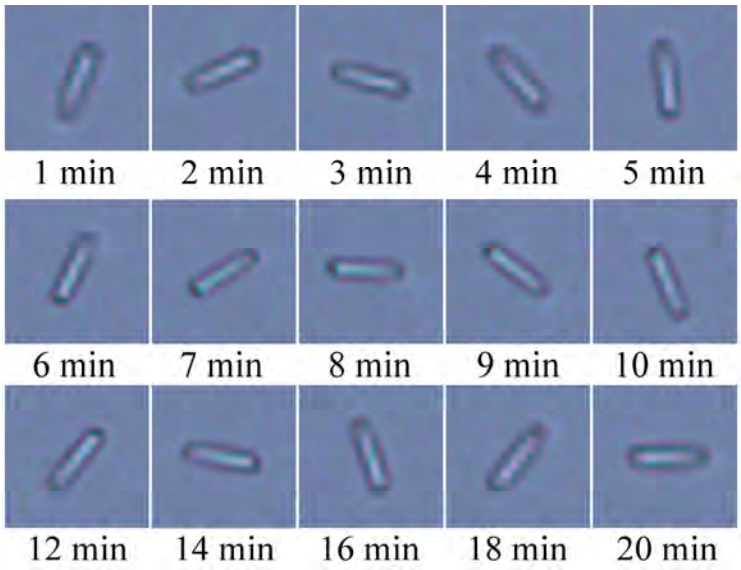

Fig. 9. A series of optical micrographs depicting the orientation of a 3 x 22 µm glass rod in a 10 µm pitch CLC cell as a function of time after it has been flipped over.

The number of degrees that the rods rotated did not correspond perfectly to the number of pitches in the cell. A possible explanation was that gravitational pull was much larger than the

#155093 - $15.00 USD Received 20 Sep 2011; revised 4 Nov 2011; accepted 4 Nov 2011; published 8 Nov 2011
(C) 2011 OSA

elastic forces within the cell, and the rod fell through portions of the cell thickness without rotation. Another possibility was that the rods never fell to the bottom substrate due to a repulsive elastic force between the flat rubbed substrate and the parallel surface anchoring on the non-flat particle. Reference [15] describes this type of phenomenon for wires with a radius of 175 nm and length of 5-35 μm in nematic liquid crystals. The glass rod positions in the z-axis of the sample were measured using laser scanning confocal microscopy. There was not enough resolution (~1 μm) to determine if the rods were sitting on the bottom substrate, but the measurements showed that glass rods were trapped within defect lines of the 2 μm and 331 nm pitch CLC samples. The odd rotation of the glass rods in the 2 μm pitch CLC sample is attributed to interactions with defect lines, and the lack of rod rotation in the 331 nm sample is due to all of the glass rods being tapped in defect lines. Figure 10 shows an x-y cross-section of the 2 μm pitch CLC, in which the glass rods were trapped in a defect line.

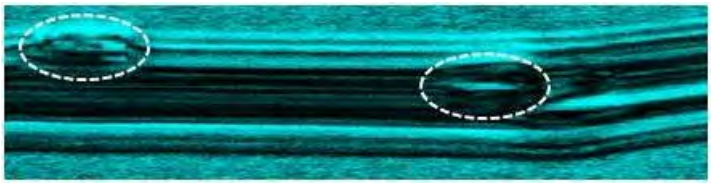

Fig. 10. A laser scanning confocal micrograph of 2 glass rods trapped in defects lines within a 2 μm pitch CLC cell.

The explanation for the loss of orientational order in the static optical micrographs as CLC pitch was decreased is not trivial because the rods dynamically follow the director orientation once the cell is flipped over. A hypothesis is that the torsional force that caused rod reorientation decreased as the pitch of the CLC decreased. As the pitch length of the CLC approaches the rod diameter, the director orientation rotates significantly over the diameter of the rod, and the torque exerted on the wire will be averaged out. There was not enough energy to rotate the glass rods into their aligned positions. However, after the cell was flipped, gravity provided the driving force necessary to reorient the rod along the LC director.

3.4 Computational results

The experimental results showed that the glass rods in CLC pitches ranging from 2 to 30 μm rotated as they fell through the cell and followed the heliocoidal rotation of the director. A computational model was created to calculate the elastic energy of the system as a function of the angle between the long axis of the glass rod and the CLC director orientation. The glass rod was allowed to orient –90° to + 90° from the CLC director. –90° and + 90° correspond to the long-axis of the glass rod taking on an orientation perpendicular to the CLC director, and 0 degrees corresponds to the long-axis of the rod taking a parallel orientation to the CLC director. For each angle between the rod and the LC at the middle plane, the LC around the rod is allowed to relax to the minimum elastic energy state. In the simulation, the ratios between the elastic constants are $K_{33}/K_{22} = 2.0$ and $K_{11}/K_{22} = 1.6$. As an example, the LC director configuration in the minimum elastic energy state on the plane perpendicular to the glass rod is shown in Fig. 11, where the cholesteric pitch is 10 μm. The minimum elastic energy as a function of rod angle was calculated for various pitch lengths and is plotted in Fig. 12.

#155093 - $15.00 USD Received 20 Sep 2011; revised 4 Nov 2011; accepted 4 Nov 2011; published 8 Nov 2011
(C) 2011 OSA

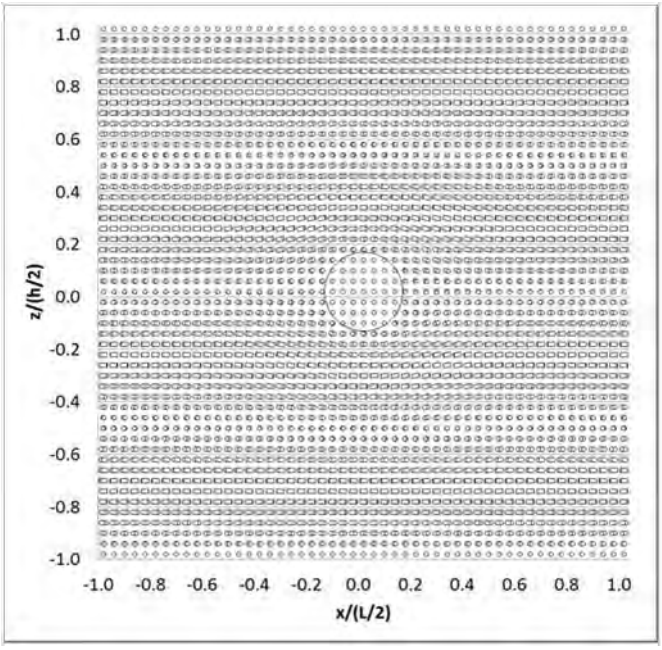

Fig. 11. Computed LC director configuration in the minimum elastic energy state when the angle between the glass rod and the LC director at the middle plane is 0°. The CLC pitch is 10 μm.

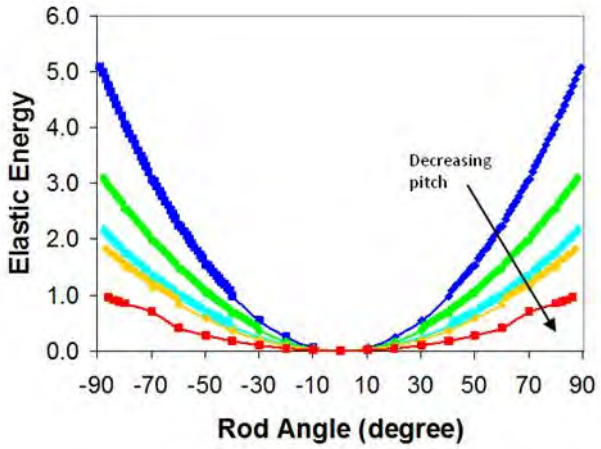

Fig. 12. Computed elastic energy (subtracted by the elastic energy at 0 degree, in units of *K22*) per unit length of glass rod as a function of angle between the long axis of the glass rod and the CLC director for CLC pitches of ∞, 20, 10, 6 and 3 μm.

The elastic energy of the system was minimized when the glass rods reoriented parallel to the LC director, but there was a greater driving force for reorientation in large pitch CLCs. At a CLC pitch of infinity, there was a large driving force for the glass rods to orient parallel to the LC director. However, at a CLC pitch of 3 μm, the driving force for rod rotation when the rod was oriented –30° to + 30° from the LC director was nearly zero. This could explain why smaller pitch CLCs do not look oriented in the optical microscope. The glass rods did not align with the LC director until the cell was flipped over, and gravity provided the force necessary or reorientation. It is interesting to note that the minimum in the elastic energy

#155093 - $15.00 USD Received 20 Sep 2011; revised 4 Nov 2011; accepted 4 Nov 2011; published 8 Nov 2011
(C) 2011 OSA

remains flat over a large number of degrees (20 degrees) which could explain why all of the rods in the 30.7 μm sample are not ordered perfectly in one direction, but rather over a range of angles.

4. Conclusion

Micron-sized glass rods align parallel to the local LC director in nematic and twisted nematic geometries. Gravity was used to sediment the rods, allowing for temporal visualization as the rods fell from the top to the bottom of differing cell architectures. The interaction of these rods in a CLC fluid of varying pitches was also explored. A computational model describing the elastic forces within the system was developed, which correctly predicts the reorientation of glass rods in the CLCs. Differences in behavior elucidated as a function of pitch dimension relative to the rod diameter were qualitatively demonstrated in the experimental behavior. Understanding the behavior of micron-sized rods in CLCs is important for applications like molecular motors, but it also provides the background necessary to create helically assembled nanorods, as a bottom-up approach for fabrication of metamaterials.

Acknowledgments

The authors wish to thank Dr. Kyungmin Lee and Dr. Michael McConney for useful discussions. This work was completed in the Materials and Manufacturing Directorate of the Air Force Research Laboratory. Funding was provided by the Air Force Office of Scientific Research and the National Research Council.